Data-Adaptive 2-D Tracking Doppler for High-Resolution Spectral Estimation

Yücel Karabiyik, Jørgen Avdal, Ingvild Kinn Ekroll, Stefano Fiorentini, Hans Torp, and Lasse Løvstakken

***Abstract*— Spectral broadening in pulsed-wave Doppler caused by the transit-time effect deteriorates the frequency resolution and may cause overestimation of maximum velocities in high-velocity blood flow regions and for large beam-to-flow angles. Data-adaptive spectral estimators have been shown to provide improved frequency resolution, especially for small ensemble lengths, but offer little or no improvement when the transit-time effect dominates. In this work, a method is presented that combines a data-adaptive spectral estimation method, the power spectral Capon, and 2-D tracking Doppler to enable improved frequency resolution for both high and low velocities. For each velocity, a time signal is extracted by tracking scatterers over time and space to decrease the transit-time effect, and power spectral Capon is used for spectral estimation. The method is evaluated using simulations, flow phantom recordings, and recordings from healthy and stenotic carotid arteries. Simulation results showed that the spectral width was decreased by 60% compared to 2-D tracking Doppler for velocities around 2.3 m/s using 12 time samples. The reduction was estimated to be 66% using the flow phantom results for 0.85-m/s mean velocity. A 5-dB SNR gain was observed from the *in vivo* results compared with Welch's method. Computer simulations confirm that in the presence of velocity gradients or out-of-plane motion, the proposed method can be used to reduce spectral broadening by requiring shorter observation windows.**

***Index Terms*— Data adaptive spectral estimators, pulsed-wave Doppler, spectral broadening.**

I. Introduction

PULSED-WAVE (PW) Doppler is an imaging modality in which the distribution of velocities inside a sample volume is estimated and displayed over time, called a spectrogram, and is the main approach used for the quantification of blood velocities. Blood velocities estimated by the delineation of spectrograms can be used for the assessment of the severity of stenosis [1] and estimation of Doppler indices such as pulsatility and resistivity index [2].

Manuscript received May 16, 2019; accepted August 19, 2019. Date of publication August 23, 2019; date of current version December 26, 2019. This work was supported by the Umoja Project—Ultrasound for Midwives in Rural Areas (Helse Midt-Norge RHF). *(Corresponding author: Yücel Karabiyik.)*

Y. Karabiyik, J. Avdal, S. Fiorentini, H. Torp, and L. Løvstakken are with the Department of Circulation and Medical Imaging, Norwegian University of Science and Technology, 7491 Trondheim, Norway (e-mail: yucel.karabiyik@ntnu.no).

I. K. Ekroll is with the Department of Circulation and Medical Imaging, Norwegian University of Science and Technology, 7491 Trondheim, Norway, and also with Kirurgisk klinikk, St. Olavs Hospital HF, 7030 Trondheim, Norway.

Digital Object Identifier 10.1109/TUFFC.2019.2937281

Conventionally, the data used for spectral estimation are extracted by transmitting successive focused pulses and sampling the backscattered signal from a fixed sample volume. The sample volume has finite dimensions determined by acquisition and beamforming parameters. As the transit time of the scatterers through the sample volume decreases, for instance, due to high scatterer velocities or out-of-plane movement, spectral broadening increases. This is referred to as transit-time broadening [3] and causes overestimation of maximum velocities if not corrected for [4]. This can result in increased intraobserver/interobserver variability and can make diagnosis more challenging [5].

Various methods have been proposed for blood velocity estimation that extract samples along the ultrasonic beam or direction of flow as opposed to a fixed location in space. A method called velocity-matched spectrum was proposed to alleviate the transit-time effect by tracking the scatterers in space to increase the observation time [6]. Focused transmissions were employed in this method and the scatterers were tracked along the beam direction. It was shown that the method could decrease the spectral broadening and suppress the velocity ambiguity in PW Doppler. However, as the tracking direction was along the beam direction, the improvement was not as substantial for large beam-to-flow angles. Later, this method was extended for tracking scatterers in 2-D, called 2-D tracking Doppler, by utilizing plane-wave transmissions and parallel beamforming [7]. It was shown that the method could reduce the spectral broadening substantially compared to the Welch [8] estimator, especially for large beam-to-flow angles and high velocities. Because the sample volume follows the scatterers over consecutive frames, the observation window has both spatial and temporal extents. Short windows limit the velocity resolution of the estimates, whereas long windows can cause violation of stationarity of flow assumption, especially when tracking high-velocity scatterers.

Methods that extract time samples along the ultrasonic beam or the flow direction to estimate the mean blood velocity also exist. A method called the butterfly search extracts samples along different delay lines called *butterfly lines* in the fast-time and slow-time space. The algorithm searches for the lowest variance among the samples based on the idea that the samples will be similar when the delay line matches the scatterer velocity [9]. Similar to the velocity-matched spectrum method, this method also extracts samples only in the radial direction. In the directional beamforming technique, the 2-D blood velocity vector is found by cross-correlating the

slow time signals along different beamforming directions [10]. Other techniques such as speckle tracking [11] and vector Doppler [12], [13] are also able to provide angle-independent velocity estimates. However, methods that rely on mean velocity estimation are more susceptible to estimation bias than spectral estimation techniques. Because of this, quantitative clinical measurements are currently based on the maximum velocity estimates. Developing more accurate spectral estimation techniques, which are less influenced by spectral- or transit-time broadening, is therefore of clinical interest.

The Welch estimator is conventionally used for spectral estimation in PW Doppler. The method is not computationally complex and can be implemented efficiently. However, it requires relatively long observation windows to achieve reasonable frequency resolution and sidelobe levels, e.g., 64–128 time samples in 5–10 ms. It is desired to keep the window length short in order to increase temporal resolution and avoid broadening due to nonstationary flow. Data-adaptive filter bank methods have been proposed to achieve high-frequency resolution with shorter window lengths. Examples include power spectral Capon [14], amplitude and phase estimation (APES) method [15], and blood iterative adaptive approach (BIAA) [16]. These methods generate a unique data-adaptive filter for the estimation of each frequency component in the spectrum to minimize the spectral leakage and achieve high temporal and frequency resolution. The methods were shown to outperform the Welch estimator for short window lengths in terms of spectral resolution. However, this improvement is observed primarily for low blood velocities [17]. The transit-time effect dominates for high velocities and large beam-to-flow angles leading to spectral broadening that is not ameliorated by adaptive estimators.

A method was proposed by the authors previously for achieving high spectral resolution for high and low velocities using a limited number of time samples in a proceeding [18]. The proposed method, referred to as tracking Capon, is a combination of 2-D tracking Doppler and the power spectral Capon where time signals are extracted from the data by tracking scatterers over consecutive frames and used as input to the Capon estimator to obtain the velocity spectrum. This work gives an in-depth analysis of the method in relevant and challenging blood velocity estimation scenarios. The performance of the method is evaluated for both out-of-plane movement and gradients in the flow field using a computational fluid dynamics (CFD) phantom. Flow phantom recordings were used to assess the method under controlled conditions, and a relevant vascular *in vivo* scenario was investigated, where both a normal and stenotic carotid artery was imaged. For all cases, the resulting spectra are compared to 2-D tracking Doppler, power spectral Capon, and the Welch method in terms of the spectral width of the estimates, i.e., spectral resolution and SNR.

The article is organized as follows. In Sections II-A and II-B, the proposed estimator and power spectral density (PSD) estimators used for comparison are presented. Data acquisitions and computer simulations that are performed to compare the tracking Capon method and existing estimators are described in Sections II-C and II-D. Spectral width comparisons, made using flow phantom, *in vivo*, and simulations with out-of-plane movement and complex flow field are given in Section III. Factors affecting the estimation quality of the tracking Capon method, its advantages and limitations, and the similarities of the tracking methods to beamforming algorithms in ultrasound imaging are discussed in Section IV. Finally, concluding remarks are given in Section V.

II. Methods

Spectral Doppler with 2-D tracking requires the acquisition of a spatial region at the Doppler pulse repetition frequency (PRF), which can be achieved by sending broader transmit beams, while utilizing parallel beamforming on receive. In this work, the data sets were recorded using plane-wave scanning schemes. The window length in this work is defined as the number of samples needed for the estimation of one spectrum excluding temporal averaging.

A. Fixed Location Sampling Estimators

Let $u(x_k, z_l, n)$ represent a sample at coordinates x_k in the lateral and z_l in the axial directions and at time index n after complex demodulation. An ensemble that has length N, i.e., window length, and acquired at this spatial point can be expressed as $\mathbf{u}(x_k, z_l, m) = [u(x_k, z_l, m), u(x_k, z_l, m+1) \cdots u(x_k, z_l, m+N-1)]^T$, where m represents the time index of the first sample.

1) Welch's Method: In this method, overlapping segments of data are used to reduce the variance, and each segment is multiplied with a window function in order to reduce the sidelobe levels. The Welch estimate may be expressed as

$$\hat{P}_{\text{Welch}}(f) = \frac{1}{KLM}\sum_{k=1}^{K}\sum_{l=1}^{L}\sum_{m=1}^{M}\left|\sum_{n=0}^{N-1} w(n)u(x_k, z_l, m+n)e^{-i2\pi fn}\right|^2 \quad (1)$$

where M is the total number of segments used, $\mathbf{w}$ is the window function, f is the normalized frequency with respect to PRF, and K and L are the number of spatial averaging points in lateral and radial directions, respectively.

2) Power Spectral Capon: The power spectral Capon estimator generates an adaptive filter that minimizes the filter output power while passing the frequency of interest undistorted. The power of the output signal after filtering with filter $\mathbf{h}_f$ is [19]

$$E[\mathbf{h}_f^{\text{H}}\mathbf{u}(x_k, z_l, m)\mathbf{u}(x_k, z_l, m)^{\text{H}}\mathbf{h}_f] = \mathbf{h}_f^{\text{H}}\mathbf{R}_{\text{Capon}}\mathbf{h}_f \quad (2)$$

where $(*)^{\text{H}}$ denotes the Hermitian transpose and $\mathbf{R}_{\text{Capon}}$ is the data covariance matrix, estimated as

$$\hat{\mathbf{R}}_{\text{Capon}} = \frac{1}{KLM}\sum_{k=1}^{K}\sum_{l=1}^{L}\sum_{m=1}^{M}\mathbf{u}(x_k, z_l, m)\mathbf{u}(x_k, z_l, m)^{\text{H}}. \quad (3)$$

The power of the output signal (2) is minimized with the constraint $\mathbf{h}_f^{\text{H}}\mathbf{a}_f = 1$, where $\mathbf{a}_f = [1\ e^{i2\pi f}\ \cdots\ e^{i2\pi f(N-1)}]^T$ is the Fourier vector and $(*)^{\text{T}}$ denotes the transpose. The resulting filter coefficients can be written as

$$\mathbf{h}_f = \frac{\hat{\mathbf{R}}_{\text{Capon}}^{-1}\mathbf{a}_f}{\mathbf{a}_f^{\text{H}}\hat{\mathbf{R}}_{\text{Capon}}^{-1}\mathbf{a}_f}. \quad (4)$$

Consequently, the filter output power in (2) is found as

$$\hat{P}_{\text{Capon}}(f) = \frac{1}{\mathbf{a}_f^{\text{H}} \hat{\mathbf{R}}_{\text{Capon}}^{-1} \mathbf{a}_f}. \tag{5}$$

B. 2-D Tracking Methods

When using 2-D tracking methods, data were extracted using 2-D spline interpolation along a given line in the image and according to a given blood velocity. For the defined beam-to-flow angle θ, an interpolated sample can be written as

$$u_\theta(r, n) = u(r \sin\theta + x_k, r \cos\theta + z_l, n) \tag{6}$$

where r is the distance from the line center $[x_k, z_l]$ to the interpolated point. Interpolation is performed for all velocities of interest along the total of KL lines. Denoting the direction of flow toward the probe as positive, a sample interpolated for velocity υ on this line after phase correction can be written as

$$u_{\theta,\upsilon,x_k,z_l}(n) = u_\theta(n\upsilon T, n_0 + n) e^{-i\omega_d n \Delta t} \tag{7}$$

where T is the pulse repetition time, n_0 is the center index in time, ω_d is the angular demodulation frequency, and

$$\Delta t = \frac{2\upsilon T \cos\theta}{c} \tag{8}$$

where c is the speed of sound in blood. Consequently, the data vector, $\mathbf{u}_{\theta,\upsilon,x_k,z_l}$, that consists of samples interpolated along this line for velocity υ can be represented as

$$\mathbf{u}_{\theta,\upsilon,x_k,z_l} = [u_{\theta,\upsilon,x_k,z_l}(-(N-1)/2), \ldots, u_{\theta,\upsilon,x_k,z_l}((N-1)/2)]^T. \tag{9}$$

1) 2-D Tracking Method: In this method, extracted signals for each line and velocity are multiplied with a windowing function $\mathbf{w}$ and summed. The estimator can be written as

$$\hat{P}_{2DT}(\upsilon) = \frac{1}{KL} \sum_{k=1}^{K} \sum_{l=1}^{L} |\mathbf{w}^{\text{T}} \mathbf{u}_{\theta,\upsilon,x_k,z_l}|^2. \tag{10}$$

Similar to the Welch method, the windowing function is used for decreasing the sidelobe levels, and a Hamming window is used in this work. Time averaging can be done by averaging $\hat{P}_{2DT}(\upsilon)$ for different n_0.

2) Tracking Capon: In the tracking Capon method, the extracted ensembles are filtered with an adaptive narrow band filter to increase the velocity resolution. The covariance matrix estimated for velocity υ using the extracted signals can be written as

$$\hat{\mathbf{R}}_\upsilon = \frac{1}{KL} \sum_{k=1}^{K} \sum_{l=1}^{L} \mathbf{u}_{\theta,\upsilon,x_k,z_l} \mathbf{u}_{\theta,\upsilon,x_k,z_l}^{\text{H}}. \tag{11}$$

The time averaging is performed by averaging the covariance matrix $\hat{\mathbf{R}}_\upsilon$ for different n_0. The estimated power is found by using the power spectral Capon estimator in (5) and the estimated covariance matrix above.

After the phase correction in (7), the interpolated time samples should be in phase when the interframe movement of the sample volume matches the velocity of the scatterers. Because of this, only the power of the zero frequency ($f = 0$) is estimated for each velocity. Finally, the proposed estimator can be given as

$$\hat{P}_{TC}(\upsilon) = \frac{1}{\sum_{i=1}^{N} \sum_{j=1}^{N} R_{ij}} \tag{12}$$

where R_{ij} represents the element of $\hat{\mathbf{R}}_\upsilon^{-1}$ in row i and column j. Fig. 1 illustrates the sampling scheme for PSD estimation. The averaging region is a grid of points moving in space and time with a defined angle. Therefore, the number of tracking lines is equal to the number of spatial points used for averaging. The resulting tracking lines have a spatial extent proportional to the velocity of interest, the length of the observation window, and the PRF.

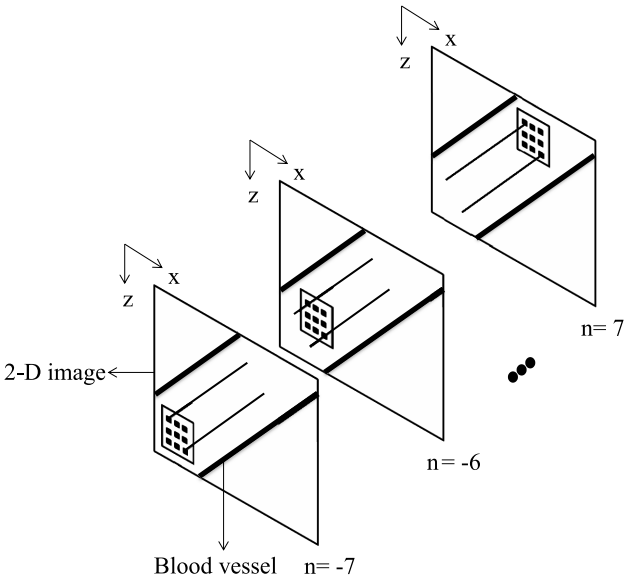

Fig. 1. Concept of extracting samples for each velocity of interest. A 2-D averaging region moves in space with a defined angle and velocity forming parallel lines ($K = 3$, $L = 3$, and $N = 15$). Two of these lines are shown in the figure.

Frequency estimates from the Welch and Capon spectral estimators were converted to velocity estimates using the Doppler equation

$$\upsilon = \frac{fc}{2 f_0 \cos\theta} \tag{13}$$

where f_0 is the center frequency of the transmit pulse.

C. Simulation Model and Parameters

A tube that had 7.5-cm length and 8-mm diameter was used as the model for the simulations. The tube had a 1.5-cm-long narrowing region in the middle. In this region, the diameter of the tube was decreased symmetrically from 8 mm down to 4 mm in the middle to simulate a stenotic region as shown in Fig. 2. The tube was centered along the main axis of the transducer at a depth of 35 mm and oriented such that the beam-to-flow angle was 70°. A stationary velocity field for the phantom was retrieved using the CFD simulation software FEniCS [20]. The flow profile within the tube was parabolic and fully developed at the inlet. The maximum velocity in the narrowing was 2.3 m/s, resulting in the maximum Reynolds number 2200. First, point scatterers were randomly placed in

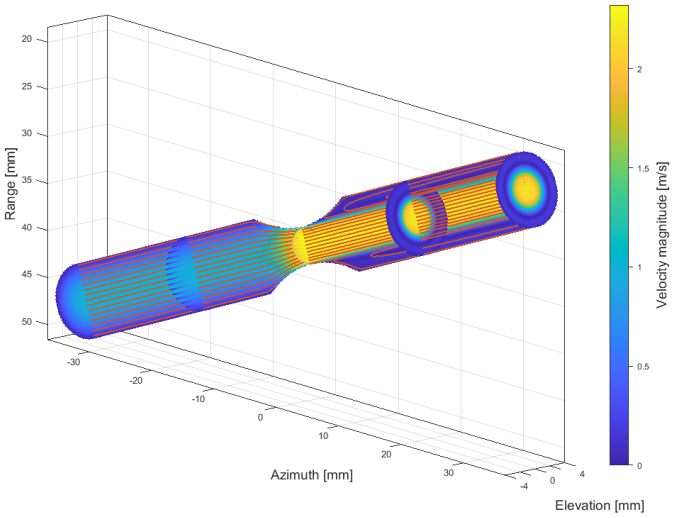

Fig. 2. Flow profile across the tube obtained with CFD simulation. The horizontal section is extracted in the middle of the tube and the cross-sectional velocity profiles are given at five different locations. The lines are the streamlines that show the paths of the moving scatterers.

TABLE I
ACQUISITION SETUP

Parameter	simulations, flow phantom & CCA	ICA
Center frequency [MHz], f_0	5	4.7
Cycles @ f_0	2.5	2.5
PRF [kHz]	4	6
Receive F-number	1.4	1.4

a rectangular box surrounding the CFD geometry. A density of ten scatterers per resolution cell was chosen to achieve fully developed speckle. Second, the velocity field was linearly interpolated at the scatterers' position, and the velocity magnitude for each scatterer was estimated. Finally, all of the scatterers with a velocity magnitude below 1 mm/s were removed. A time-dependent velocity field was obtained by multiplying the stationary velocity field with the positive half-cycle of 1-Hz sinusoidal function. Fig. 2 shows the simulated flow field across the tube and at five different cross sections when the velocities are maximum. The Field II [21], [22] simulation software was used to generate the received ultrasound signals. The simulation parameters are given in Table I. Two different sets of data were simulated using the described CFD phantom, as shown in Fig. 2: one where the imaging plane was aligned with the direction of the flow, and the second where the phantom was rotated 15° about the z-axis. The simulated data sets were thus used with the proposed tracking Capon and the 2-D tracking Doppler methods to demonstrate the effects of velocity gradients in the flow field and out-of-plane movement. Spectral estimation was performed for 512 velocities equally spaced between 0 and 4 m/s.

D. Data Acquisition and Processing

Performance of the method was further assessed using a flow rig [7] and two *in vivo* recordings. One of the recordings was from common carotid artery (CCA) of a healthy volunteer [7] and the other was from a volunteer with a stenosis in the internal carotid artery (ICA) [23]. Table I summarizes the acquisition parameters. Plane-wave transmissions were used, with beam-to-flow angles of 70°, 68°, and 62° for the healthy volunteer, volunteer with stenotic artery, and flow phantom, respectively. Plane waves were transmitted with a 10° transmit angle, and the parallel receive beamforming angle was matched to the transmit angle. The PRFs were chosen to give high temporal resolution and avoid a large degree of aliasing.

TABLE II
POSTPROCESSING PARAMETERS

Parameter	flow phantom	simulations	CCA	ICA
Averaging area [mm]	1.5 × 1.5	1.2 × 0.6	1.4 × 0.6	0.16 × 0.15
Temporal averaging [ms]	10	10	10	8
Tracking length [cm]	0.43	1.1	0.75	0.73
Window length, N	16	12	16	12

A SonixMDP ultrasound system (Ultrasonix, Richmond, BC, Canada) with a 5-MHz linear probe was used for recordings of flow phantom and the CCA of the healthy volunteer. The flow phantom (Model 524 Peripheral Vascular Doppler Flow Phantom, ATS Laboratories, Bridgeport, CT, USA) consisted of a tissue-mimicking material surrounding a straight tube. The PhysioPulse 100 flow system (Shelley Medical Image Technologies, London, ON, Canada), pumping blood-mimicking fluid, was connected to the flow phantom to form a flow loop. The system was set to give 1-Hz sinusoidal flow with a positive offset.

The volunteer with stenosis was imaged using a Verasonics ultrasound system (Verasonics Inc., Redmond, WA, USA) with an L11-4V linear probe. The sample volume was placed in the stenotic region in the ICA.

The acquired data were clutter filtered using a 51-order finite-impulse response (FIR) filter with a normalized cutoff frequency at 0.1π rad/sample. Beam-to-flow angles for the 2-D tracking Doppler and tracking Capon methods were chosen by using the color flow images as a guide to select a tentative angle. Later, spectrograms were generated for several angles around the tentative angle, and the angle with the minimum spectral broadening was chosen as the tracking angle.

The tracking methods can suppress the velocity ambiguity, which makes it possible to distinguish the true velocity trace from the aliased. The aliased and the true velocity can be distinguished by their spectral widths and power, i.e., the true velocity trace has reduced spectral width and higher spectral power. The Nyquist velocity or ±PRF was not taken into account for the display of the spectrograms. The velocity range was chosen to give a good interpretation of the true and the aliased velocity traces. For the tracking methods, spectral estimates were done for equally spaced 512 velocities between ±2 and ±1.15 m/s for CCA and flow phantom results, respectively. The velocity range was 0–4 m/s for the stenotic artery and simulation results. The Welch and Capon PSD estimates were done using 512 frequency points, and spectrograms were stacked to obtain the same velocity limits as the tracking methods for comparison purpose. The postprocessing parameters used for the generation of the results are given in Table II. The window length, N, does not include samples used for temporal averaging.

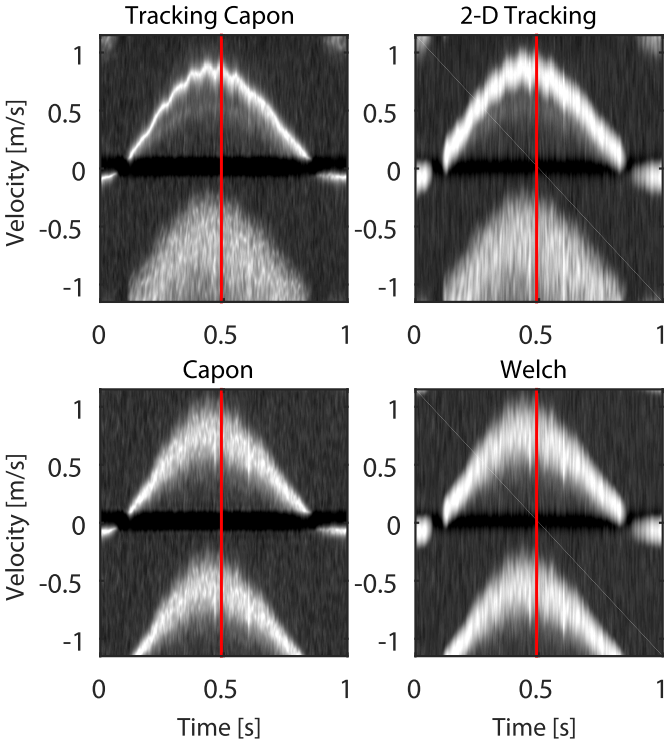

Fig. 3. Spectrograms generated using tracking Capon, 2-D tracking Doppler, Capon, and Welch methods using the flow phantom recording. The beam-to-flow angle is 62°. The dynamic range used for display is 40 dB.

III. Results

A. Flow Phantom Results

Fig. 3 shows a comparison among the proposed method, 2-D tracking Doppler, power spectral Capon, and Welch's method using data from the flow phantom recording. Averaging was done over a 1.5 mm × 1.5 mm spatial region and a 10-ms temporal window. The observation window length was set to 16 samples for all methods. This resulted in a maximum tracking length of 0.43 cm, corresponding to the highest investigated velocity of 1.15 m/s. As can be observed, the proposed method yields spectrograms with reduced spectral broadening for low and high velocities compared to other methods. This can be observed from the leakage into the stopband of the clutter filter due to the low sidelobe suppression capabilities of the Welch and 2-D tracking methods for short window lengths. The Capon method yielded higher resolution estimates than the 2-D tracking Doppler and the Welch methods for low velocities. However, both the Welch and Capon spectra had similar spectral width for high velocities, while 2-D tracking Doppler method could decrease the transit-time broadening.

Fig. 4 shows spectra corresponding to the red vertical lines in the spectrograms in Fig. 3, where the mean velocity is approximately 0.85 m/s. The spectral width at −3 dB was found to be approximately 5, 15, 26, and 32 cm/s for this mean velocity for the proposed method, 2-D tracking, Capon, and Welch methods, respectively. Fig. 4 also shows that tracking results in suppression (decreased power) of the aliased part of the spectrum and increased SNR.

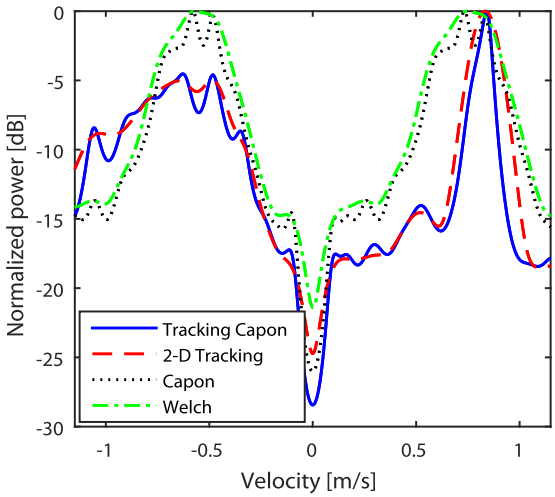

Fig. 4. Doppler power spectra from the flow phantom recording, corresponding to the time instances marked with red lines in Fig. 3.

B. Simulation Results

Fig. 5 (top) shows the velocity field in the middle of the CFD phantom when the velocities are highest. The imaging plane is in the middle of the tube and aligned with the flow direction. The spectra were generated from two different regions: prestenosis (denoted as 1) and mid-stenosis (denoted as 2), which are marked with red squares on the velocity field. The tracking length for the highest velocity present, 2.3 m/s, was 0.63 cm (white line) for a 12-sample window and 1.78 cm (black line) for a 32-sample window. The extent of the averaging region used for estimations was 1.2 mm × 0.6 mm in lateral and radial directions, respectively. A 10-ms time window was used for temporal averaging.

Spectrograms in the left column were estimated using the data from the prestenosis region. As can be seen, the tracking Capon method with an observation 12-sample window yielded spectral estimates with reduced broadening compared to the 2-D tracking Doppler for the same window length. Increasing the window length improved the spectral resolution for the 2-D tracking Doppler for velocities up to 0.6 m/s. For higher velocities, the spectral width increased due to the higher velocities present in the flow field toward the stenosis.

The spectrograms estimated using the data from the mid-stenosis region are shown in the right column of Fig. 5. Higher velocities are present in this region compared to the prestenosis region. Similar to the prestenosis region, the proposed method could decrease spectral broadening further than 2-D tracking Doppler for a window length of 12 and 32 samples. The spectral width at −3 dB was 9 and 22.7 cm/s for tracking Capon and 2-D tracking Doppler, respectively, with a window length of 12 samples, which corresponds to a 60% reduction. It can again be seen that increased tracking length resulted in increased spectral broadening due to the velocity gradients in the flow field. The velocity gradients also caused a decrease in the signal power for the proposed method for high velocities (>2 m/s) due to lost signal coherency.

Fig. 6 shows the effect of out-of-plane movement. The results are generated using data from the mid-stenosis region in Fig. 5, where the CFD phantom was rotated by 15° as

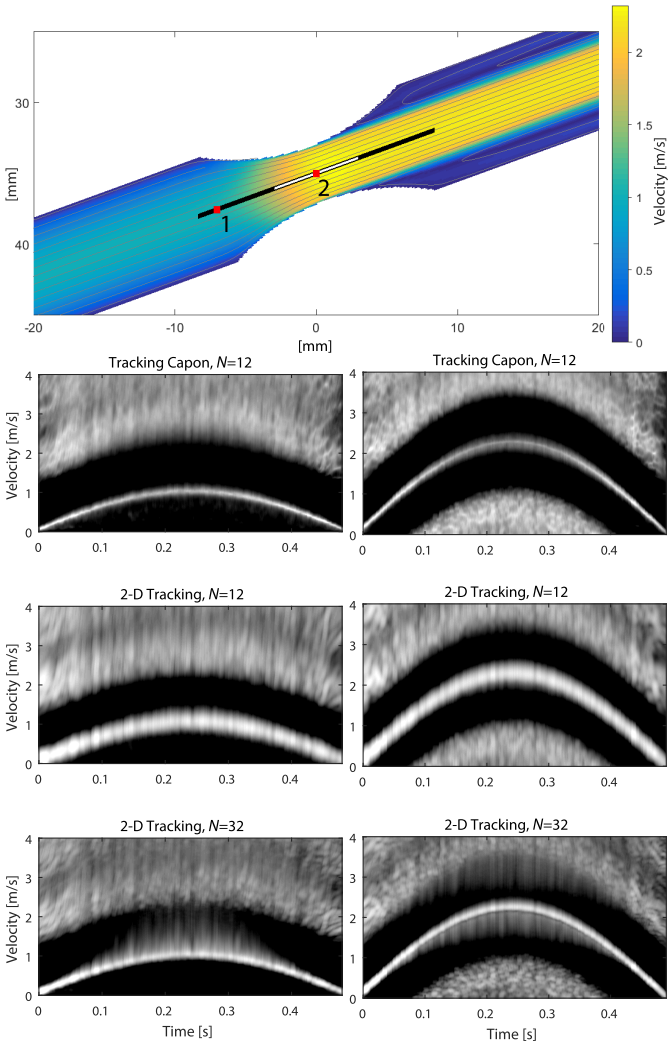

Fig. 5. Top: velocity field in the middle of the tube. The red squares denote the middle of the tracking lines, where data are extracted from prestenosis region (denoted as 1) and mid-stenosis region (denoted as 2). The lines show the tracking lengths for observation window lengths 12 (white) and 32 (black) samples for velocity 2.3 m/s. The spectrograms on the left panel show the prestenosis region results for the proposed method with a 12-sample window and 2-D tracking Doppler with window lengths 12 and 32 samples, while the right panel spectrograms show the results for data extracted from mid-stenosis region. The beam-to-flow angle was 70° and the dynamic range used for the display of the spectrograms was 40 dB.

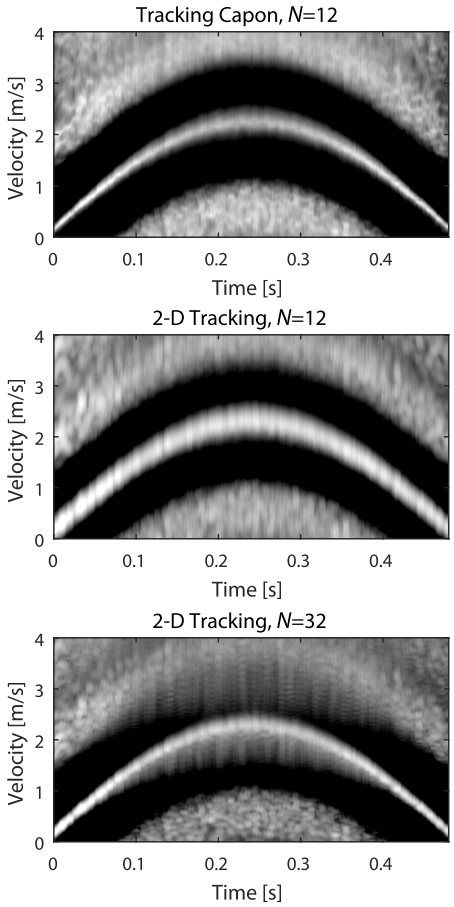

Fig. 6. Effect of out-of-plane flow movement on the tracking methods. The data are extracted from the same mid-stenosis region denoted as 2 in Fig. 5. The beam-to-flow angle was 70° and the dynamic range used was 40 dB.

explained in Section II-C. It is seen that tracking Capon outperforms 2-D tracking Doppler for window length 12. Increasing the window length up to 32 increased spectral broadening for high velocities due to out-of-plane movement. However, compared to the in-plane-flow case, shown in the left column of Fig. 5, the spectral broadening is increased for both methods and window lengths.

C. In Vivo Results

Spectrograms generated using the recording from the CCA of a healthy volunteer are shown in Fig. 7. The 2-D averaging region has dimensions of 1.4 mm × 0.6 mm in lateral and radial directions, respectively. The maximum tracking length which was required for 2 m/s was 0.75 cm. There is a clear reduction in spectral broadening for the proposed method, especially for high velocities, e.g., peak systolic velocity.

The upper panel in Fig. 8 shows spectra corresponding to the red vertical lines in Fig. 7, while the lower panel corresponds to the green lines. The mean velocities for the time instants are approximately 0.2 and 1 m/s for the red and green lines, respectively. The proposed method provides the best spectral resolution for both low and high velocities. The aliased part of the tracking Capon and 2-D tracking spectra has lower power compared to other methods, and the proposed method could decrease the sidelobe levels even further than the 2-D tracking Doppler method in this case. A 5-dB SNR gain can be observed for the tracking methods compared to the Welch and Capon methods.

Fig. 9 shows the spectrograms from the stenotic ICA. The data are extracted from the region of highest in-plane velocity. As can be seen, the tracking Capon decreases the spectral broadening compared to the Welch and Capon methods with the window length of 12 and 2-D tracking Doppler with the window lengths of 12 and 32. The power of the aliased part was significantly lower for the proposed method. The clutter filtering effect, seen as dark bands around twice the Nyquist velocity in the Welch and Capon methods, is not observed in the tracking methods.

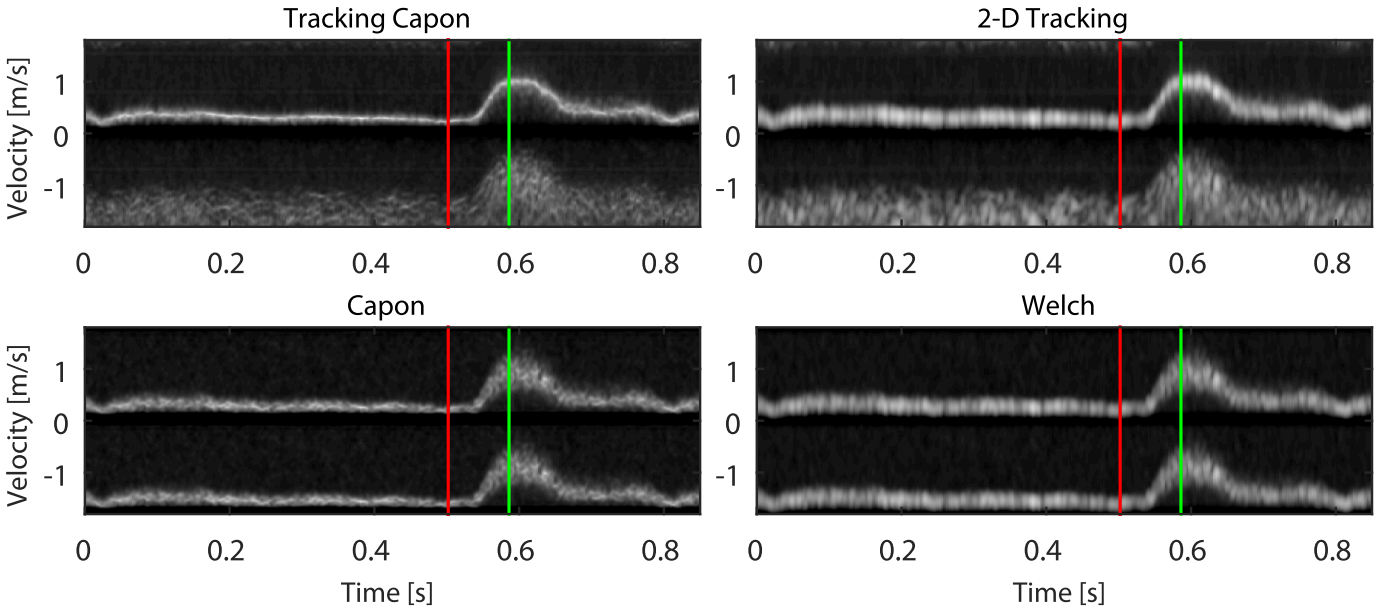

Fig. 7. Spectrograms that are generated with tracking Capon, 2-D tracking Doppler, Capon, and Welch's methods using *in vivo* recording. The beam-to-flow angle is 70°. The dynamic range used for display is 40 dB.

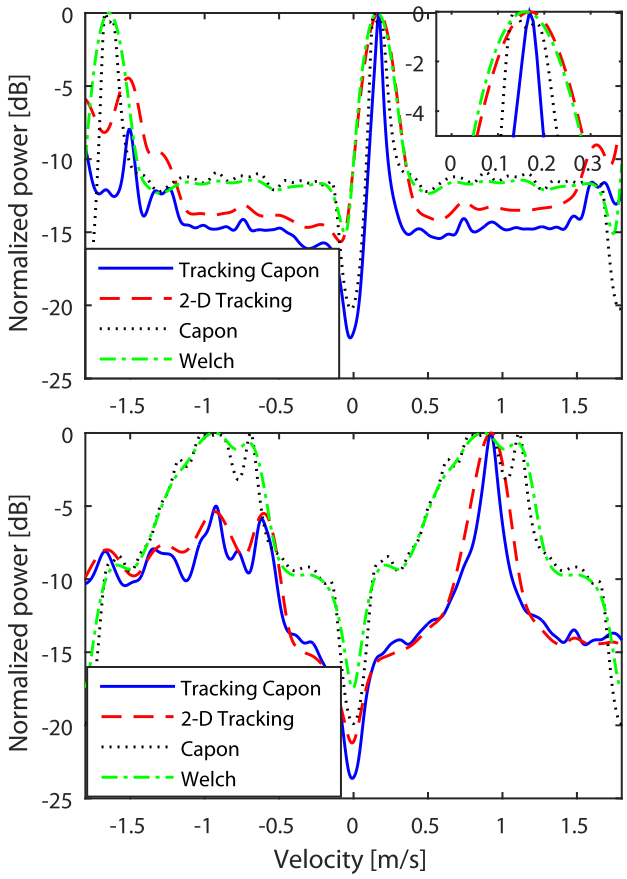

Fig. 8. Top and bottom: velocity spectra corresponding to the time instances marked in Fig. 7 with red and green lines, respectively.

IV. Discussion

A data-adaptive spectral estimator has been proposed to decrease spectral broadening even when utilizing a limited number of temporal samples. The estimator is a combination of the power spectral Capon and 2-D tracking Doppler: time samples are extracted as in the tracking Doppler corresponding to each velocity component, while the spectral power estimation is done with the Capon estimator. The *in vivo* and flow phantom results showed that for a limited number of time samples, the proposed data-adaptive method could reduce spectral broadening further than what can be achieved with the 2-D tracking Doppler. The simulation results confirmed that broadening in the tracking Doppler spectra due to spatial velocity gradients can be reduced when the length of the observation window is decreased. The addition of the Capon estimator can then be used to regain the spectral resolution.

The use of data-adaptive spectral estimators can by itself decrease spectral broadening with short window lengths (e.g., ∼16) for low velocities as shown for the Capon estimator in Figs. 3 and 8 (top). However, for high velocities, increased spectral broadening is inevitable when the spectral broadening due to transit-time effect dominates as shown in Fig. 4. The transit-time effect is alleviated by increasing the observation time of the scatterers in the tracking methods. Another advantage of increased observation time is the improved SNR. When the scatterer velocity matches the tracking velocity, extracted samples match in phase and amplitude resulting in increased signal power (Figs. 4 and 8). However, factors that reduce the signal coherency (e.g., velocity gradients and turbulent flow) can potentially decrease the signal power and increase the spectral broadening and variance of the estimates.

Both tracking Capon and 2-D tracking Doppler methods are based on tracking the spatial movement of scatterers in order to increase the observation time. However, in the tracking Capon technique, a data-dependent filter with zero-center frequency is also generated, which results in the suppression of interfering velocity components and decreases spectral broadening. More insights into how methods work can be gained by looking at

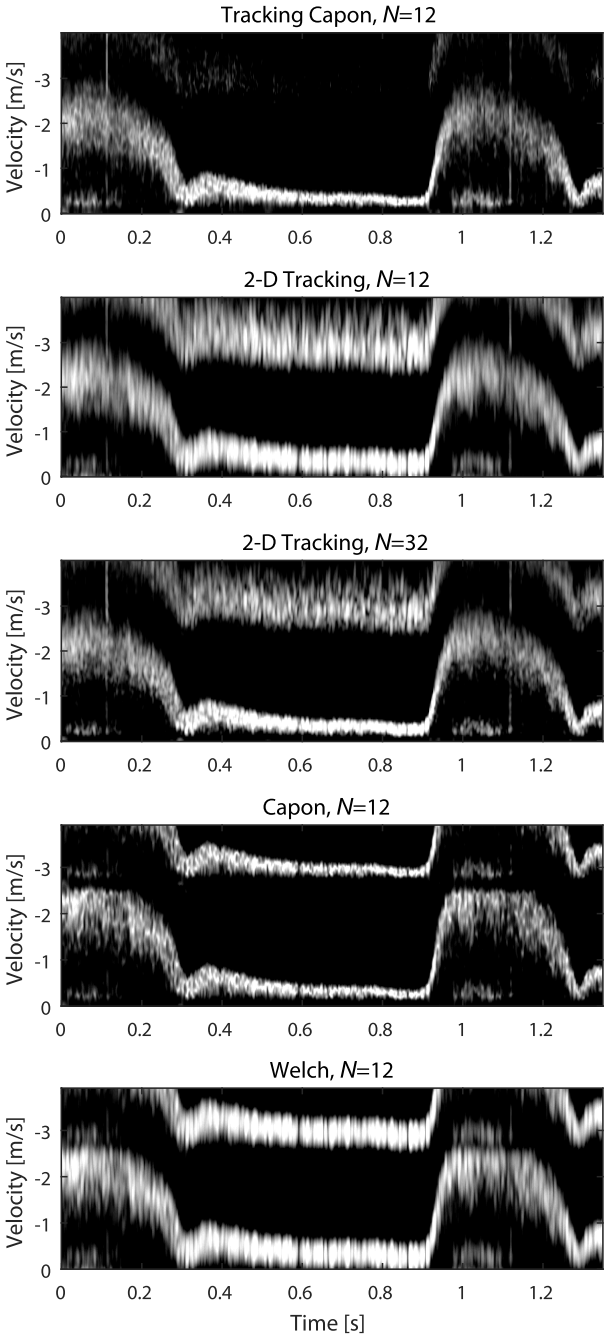

Fig. 9. Spectrograms generated using *in vivo* recording from ICA. The Nyquist velocity is 1.3 m/s. The data were extracted from the mid-stenotic region in the artery. The beam-to-flow angle was 68° and the dynamic range used for the display of the spectrograms was 30 dB.

beamforming algorithms, as the problem formulation and the solution of tracking methods share similarities with beamforming in ultrasound imaging. In delay-and-sum beamforming [24], signals received by the transducer elements are sampled at a time instant defined by the delay times generated for a specific point in space. After delaying the signals and sampling, all samples are assumed to be coherent and summed after multiplying with a defined apodization window function. This is similar to 2-D tracking Doppler where samples are summed coherently after multiplying with a window function. However, the delay lines are, here, determined by the velocity of interest, flow direction, and the PRF. The Capon beamformer [25] further estimates a windowing function depending on the received data to suppress the echoes coming from the directions other than the direction of interest. In the case of velocity estimation, the samples are multiplied with a window that suppresses velocities other than the velocity of interest, which is the zero velocity after spatiotemporal alignment. However, in the beamforming problem, the amplitude is of interest, whereas in the spectral estimation, power is sought and therefore spectral power Capon is employed.

The advantage of achieving improved frequency resolution with reduced observation window size is demonstrated in Fig. 5 (left), where the required tracking length for 2-D tracking Doppler results in spectral broadening and increased maximum velocities due to the inclusion of high velocities from the stenotic region. Similarly, in the mid-stenosis region [Fig. 5 (right)], the required tracking length yields spectral broadening toward lower velocities.

There are several factors that can decrease the frequency resolution improvement achieved by the proposed method. Figs. 5 and 6 show that out-of-plane movement results in spectral broadening both for the 2-D tracking Doppler and the proposed tracking Capon technique. The broadening is most apparent for high velocities using the 2-D tracking method with $N = 32$ due to increased tracking length.

Another possible source of error for tracking methods is incorrect beam-to-flow angle estimation, which results in broadening of the main lobe and decreased signal power [26]. Moreover, the flow angle may change due to complex flow fields. The flow angle is more likely to change within the observation window when tracking high-velocity scatterers and/or when the number of samples used for velocity estimation is high as both situations result in increased tracking length in space.

All methods were evaluated with data recorded from a stenotic ICA to investigate the performance of the methods in a clinically relevant, high-velocity condition. It was seen that the spectral broadening could be decreased using the proposed method and 2-D tracking method with an observation window length of 32. The proposed method could improve the spectral resolution further in low-velocity regions. In addition, the dropout in the fixed location sampling methods around twice the Nyquist velocity is not observed when using the tracking methods. The improvement in spectral broadening was limited for high velocities in the stenotic artery case, compared to the healthy CCA (Fig. 7). This might be due to changing flow direction throughout the cardiac cycle, the inherent complexity of the flow field itself, out-of-plane motion, or a combination of these factors.

A disadvantage of tracking Capon compared to the 2-D tracking Doppler is that it requires a larger spatial averaging region to generate robust estimates due to the need of avoiding ill-conditioned covariance matrix when inversion is applied. This may increase spectral broadening due to velocity gradients in the averaging region. Employing both temporal and spatial averaging decreases the dependence on spatial averaging. However, temporal and spatial averaging need to be designed carefully in order to adhere to the stationarity

assumption. In addition, the matrix inversion increases the number of operations needed for tracking Capon estimates, and the estimator is computationally more expensive than the 2-D tracking Doppler. However, reduced tracking length alleviates this problem as less samples are needed to estimate the spectral power.

The tracking angles were chosen manually by visual inspection of the color flow images as well as generating spectrograms with different beam-to-flow angles and choosing the ones with the minimum spectral broadening. However, the method can be improved by employing an automatic angle estimator that estimates the beam-to-flow angle either once for all spectral estimations or by updating the angle for each time sample extraction to follow scatterers in curved paths as proposed in [23] for the 2-D tracking Doppler method.

Quantitative Doppler analysis with mean velocity estimators is challenging due to several reasons. Mean velocity estimators such as the autocorrelation method [27] used in color flow imaging are angle-dependent and sensitive to leakage from the clutter filters and clutter filter settings, which can lead to underestimation or overestimation of maximum velocities and high variance in the estimates [28]. However, they can be used for the detection of regions with blood flow, turbulence, and backward flow, or for assisting sample volume placement in PW Doppler [29]. Angle-independent estimators such as the vector Doppler have been proposed to be used for quantitative Doppler analysis [13]. However, similar to the autocorrelation method, clutter and clutter filters can cause a bias when determining peak velocities. Another method called Doppler frequency spatial analysis method [30], which can be seen as a combination of PW Doppler and color flow imaging proposed to cancel intrinsic broadening in spectral Doppler, provides a histogram of mean velocities in a defined region of interest. The performance of this method is also dependent on the quality of mean velocity estimates, and the method may underestimate maximum velocities when the velocity gradients are large compared to the resolution in the image which may be the case in complex flow fields. The improved resolution achieved by the proposed tracking Capon estimator can make delineation of the true maximum velocities easier which is crucial for applications such as diagnosis of stenosis in arteries or Doppler index calculation in obstetrics. However, as demonstrated previously, the user has to ensure the correct beam-to-flow angle and avoid out-of-plane movement in order to achieve decreased spectral broadening.

V. Conclusion

A method for improving the Doppler spectral resolution while reducing spectral broadening for short observation windows was presented. The tracking Capon method combines 2-D tracking to increase the scatterer observation time and the power spectral Capon estimator to improve the spectral resolution. The proposed method could yield spectra with considerably higher frequency resolution, especially for high velocities. A 60% reduction in spectral broadening was achieved compared to 2-D tracking Doppler for 2.3-m/s mean velocity and with 70° beam-to-flow angle. Although the method requires straight-line flow and signal decorrelation can affect the performance of the method, being able to produce high-resolution PSDs with short observation window lengths can potentially extend the use of 2-D tracking concept to complex flow fields with rapid accelerations.

Acknowledgment

The authors would like to thank F. E. Fossan for his help with the generation of the simulation model and T. D. Fredriksen for sharing the flow phantom data.

References

[1] W. M. Blackshear, D. J. Phillips, P. M. Chikos, J. D. Harley, B. L. Thiele, and D. E. Strandness, Jr., "Carotid artery velocity patterns in normal and stenotic vessels," *Stroke*, vol. 11, no. 1, pp. 67–71, 1980.

[2] J. S. Cnossen *et al.*, "Use of uterine artery Doppler ultrasonography to predict pre-eclampsia and intrauterine growth restriction: A systematic review and bivariable meta-analysis," *Can. Med. Assoc. J.*, vol. 178, no. 6, pp. 701–711, 2008.

[3] V. L. Newhouse, P. J. Bendick, and W. Varner, "Analysis of transit time effects on Doppler flow measurement," *IEEE Trans. Biomed. Eng.*, vol. BME-23, no. 5, pp. 381–387, Sep. 1976.

[4] P. Tortoli, G. Guidi, and V. L. Newhouse, "Improved blood velocity estimation using the maximum Doppler frequency," *Ultrasound Med. Biol.*, vol. 21, no. 4, pp. 527–532, 1995.

[5] E. Y. L. Lui, A. H. Steinman, R. S. C. Cobbold, and K. W. Johnston, "Human factors as a source of error in peak Doppler velocity measurement," *J. Vascular Surg.*, vol. 42, pp. 972-e1–972-e10, Nov. 2005.

[6] H. Torp and K. Kristoffersen, "Velocity matched spectrum analysis: A new method for suppressing velocity ambiguity in pulsed-wave Doppler," *Ultrasound Med. Biol.*, vol. 21, no. 7, pp. 937–944, 1995.

[7] T. D. Fredriksen, I. K. Ekroll, L. Lovstakken, and H. Torp, "2-D tracking Doppler: A new method to limit spectral broadening in pulsed wave Doppler," *IEEE Trans. Ultrason., Ferroelectr., Freq. Control*, vol. 60, no. 9, pp. 1896–1905, Sep. 2013.

[8] P. D. Welch, "The use of fast Fourier transform for the estimation of power spectra: A method based on time averaging over short, modified periodograms," *IEEE Trans. Audio Electroacoust.*, vol. AU-15, no. 2, pp. 70–73, Jun. 1967.

[9] S. K. Alam and K. J. Parker, "The butterfly search technique for estimation of blood velocity," *Ultrasound Med. Biol.*, vol. 21, no. 5, pp. 657–670, 1995.

[10] J. A. Jensen and N. Oddershede, "Estimation of velocity vectors in synthetic aperture ultrasound imaging," *IEEE Trans. Med. Imag.*, vol. 25, no. 12, pp. 1637–1644, Dec. 2006.

[11] L. N. Bohs, B. J. Geiman, M. E. Anderson, S. C. Gebhart, and G. E. Trahey, "Speckle tracking for multi-dimensional flow estimation," *Ultrasonics*, vol. 38, nos. 1–8, pp. 369–375, Mar. 2000.

[12] I. K. Ekroll, T. Dahl, H. Torp, and L. Løvstakken, "Combined vector velocity and spectral Doppler imaging for improved imaging of complex blood flow in the carotid arteries," *Ultrasound Med. Biol.*, vol. 40, no. 7, pp. 1629–1640, Jul. 2014.

[13] P. Tortoli, M. Lenge, D. Righi, G. Ciuti, H. Liebgott, and S. Ricci, "Comparison of carotid artery blood velocity measurements by vector and standard Doppler approaches," *Ultrasound Med. Biol.*, vol. 41, no. 5, pp. 1354–1362, May 2015.

[14] J. Capon, "High-resolution frequency-wavenumber spectrum analysis," *Proc. IEEE*, vol. 57, no. 8, pp. 1408–1418, Aug. 1969.

[15] F. Gran, A. Jakobsson, and J. A. Jensen, "Adaptive spectral Doppler estimation," *IEEE Trans. Ultrason., Ferroelectr., Freq. Control*, vol. 56, no. 4, pp. 700–714, Apr. 2009.

[16] E. Gudmundson, A. Jakobsson, J. A. Jensen, and P. Stoica, "Blood velocity estimation using ultrasound and spectral iterative adaptive approaches," *Signal Process.*, vol. 91, no. 5, pp. 1275–1283, 2011.

[17] I. K. Ekroll, H. Torp, and L. Lovstakken, "Spectral Doppler estimation utilizing 2-D spatial information and adaptive signal processing," *IEEE Trans. Ultrason., Ferroelectr., Freq. Control*, vol. 59, no. 6, pp. 1182–1192, Jun. 2012.

[18] Y. Karabiyik, J. Avdal, I. K. Ekroll, H. Torp, and L. Løvstakken, "Data adaptive 2-D tracking Doppler," in *Proc. IEEE Int. Ultrason. Symp. (IUS)*, Sep. 2016, pp. 1–4.

[19] P. Stoica *et al.*, *Spectral Analysis of Signals*, vol. 1. Upper Saddle River, NJ, USA: Prentice-Hall, 2005.

[20] M. Alnæs *et al.*, "The FEniCS project version 1.5," *Arch. Numer. Softw.*, vol. 3, no. 100, pp. 9–23, 2015.

[21] J. A. Jensen, "Field: A program for simulating ultrasound systems," in *Proc. 10th Nordicbaltic Conf. Biomed. Imag.*, vol. 4, 1996, pp. 351–353.

[22] J. A. Jensen and N. B. Svendsen, "Calculation of pressure fields from arbitrarily shaped, apodized, and excited ultrasound transducers," *IEEE Trans. Ultrason., Ferroelectr., Freq. Control*, vol. 39, no. 2, pp. 262–267, Mar. 1992.

[23] J. Avdal, L. Løvstakken, H. Torp, and I. K. Ekroll, "Combined 2-D vector velocity imaging and tracking Doppler for improved vascular blood velocity quantification," *IEEE Trans. Ultrason., Ferroelectr., Freq. Control*, vol. 64, no. 12, pp. 1795–1804, Dec. 2017.

[24] K. E. Thomenius, "Evolution of ultrasound beamformers," in *Proc. IEEE Ultrason. Symp.*, vol. 2, Nov. 1996, pp. 1615–1622.

[25] J. F. Synnevag, A. Austeng, and S. Holm, "Adaptive beamforming applied to medical ultrasound imaging," *IEEE Trans. Ultrason., Ferroelectr., Freq. Control*, vol. 54, no. 8, pp. 1606–1613, Aug. 2007.

[26] T. D. Fredriksen, J. Avdal, I. K. Ekroll, T. Dahl, L. Lovstakken, and H. Torp, "Investigations of spectral resolution and angle dependency in a 2-D tracking Doppler method," *IEEE Trans. Ultrason., Ferroelectr., Freq. Control*, vol. 61, no. 7, pp. 1161–1170, Jul. 2014.

[27] C. Kasai, K. Namekawa, A. Koyano, and R. Omoto, "Real-time two-dimensional blood flow imaging using an autocorrelation technique," *IEEE Trans. Sonics Ultrason.*, vol. SU-32, no. 3, pp. 458–464, May 1985.

[28] B. Griewing, C. Morgenstern, F. Driesner, G. Kallwellis, M. L. Walker, and C. Kessler, "Cerebrovascular disease assessed by color-flow and power Doppler ultrasonography: Comparison with digital subtraction angiography in internal carotid artery stenosis," *Stroke*, vol. 27, no. 1, pp. 95–100, 1996.

[29] J. M. de Bray *et al.*, "Colour Doppler and duplex sonography and angiography of the carotid artery bifurcations," *Neuroradiology*, vol. 37, no. 3, pp. 219–224, 1995.

[30] B.-F. Osmanski, J. Bercoff, G. Montaldo, T. Loupas, M. Fink, and M. Tanter, "Cancellation of Doppler intrinsic spectral broadening using ultrafast Doppler imaging," *IEEE Trans. Ultrason., Ferroelectr., Freq. Control*, vol. 61, no. 8, pp. 1396–1408, Aug. 2014.